University of Baghdad
College of Engineering
JE
JOURNAL OF ENGINEERING

Journal of Engineering

journal homepage: www.jcoeng.edu.iq

Volume 32 Number 5 May 2026

Crosslinked Gelatin for Sunset Yellow Dye Removal: Synthesis, Characterization, and Adsorption Performance

Haya Musab [1, *], **Mahmmod Al-Mashhadani** [1], **Sanaa Al-Sahib** [2]

[1]Department of Chemical Engineering, College of Engineering, University of Baghdad, Baghdad, Iraq
[2]Department of Chemistry, College of Science for Women, University of Baghdad, Baghdad, Iraq

ABSTRACT

Gelatin is a valuable substance that is known to have a complex 3D structure, but it has limited adsorption efficiency, which limit its application at physiological temperature. In this paper, gelatin was improved by the addition of glutaraldehyde (GTA) to enhance its ability to adsorb dye in aqueous solution. The adsorption experiments were conducted under different conditions, such as the amount of adsorbent, the concentration of the dye, and the temperature. The study found that the q_e by GTA-GE (4.978 to 23.056 mg/g) and GE (4.8 to 21.333 mg/g) increased with the increase of initial dye concentrations but decreased with the amount of adsorbent. The parameters at equilibrium were at a pH of 4 and a dose of adsorbent of 100 mg in a time of 80 minutes. The dye removal efficiency ranged from 88.4 to 99.8 % for GTA-GE and 83 to 96 % for GE. The equilibrium data showed that Freundlich gave the best fit(R^2 = 0.995), showing a heterogeneous with multilayer adsorption. The kinetics of SY adsorption on gelatin were in pseudo-second order(R^2=0.981), which represents a good sorption process. Thermodynamic analysis showed that the negative value of ΔG indicates that the process is spontaneous and possible, whereas the negative value of ΔH (-12.693 kJ/mol) means adsorption is exothermic. Negative value of ΔS (-0.021 kJ/mole.K) implies that the decrease in randomness at the solid-liquid interface rises at the time of the adsorption process. The adsorbent can be reused four times with only a slight decrease in the removal.

Keywords: Gelatin, Adsorption, Sunset yellow, Kinetics, Glutaraldehyde.

1. INTRODUCTION

Clean water is a very important part of human existence that ensures sustainable development and maintenance of the health of ecosystems **(Chen et al., 2021)**. The United Nations World Water Development Report estimates that about 359 billion cubic meters of wastewater are produced annually around the globe, of which only 64% is treated. This

*Corresponding author
Peer review under the responsibility of University of Baghdad.
https://doi.org/10.31026/j.eng.2026.05.08

Article received: 25/02/2026
Article revised: 19/04/2026
Article accepted: 22/04/2026
Article published: 01/05/2026

leaves 36 % without treatment **(Al-Bayati et al., 2025)**. Wastewater commonly includes food colors, cosmetics, paper, and plastic **(Tkaczyk et al., 2020)**. Food dyes exhibit some economically key features, such as cost-effectiveness, light and pH stability, and improved color stability. Most of these dyes are azo compounds and produce synthetic dyes that have coal tar derivatives (e.g., sunset yellow dye)**(Dey and Nagababu, 2022)**. However, the presence of this pollutant in soil, surface water, and groundwater even at a low level is the most observable sign of water pollution **(Mohammed et al., 2023)**. Special organic pollutants can lead to poisoning of aquatic life, toxicity, and may result in genetic mutations in aquatic organisms **(Moghaddam and Seyyedi, 2022)**. Sunset Yellow (SY) is an azo-based synthetic dye. It is water-soluble and has slight solubility in ethanol; its IUPAC name is disodium 6-hydroxy-5-(4-sulfonatophenyl) diazenyl naphthalene-2-sulfonate. This compound finds extensive applications as a colorant in several industries, such as food, pharmaceutical, cosmetic, textile, and the leather industry **(Hiawi and Ali, 2023)**. Overexposure to food dyes in children can result in allergic reactions, hyperactivity, and attention deficit disorders. Dyes are complex in structure and chemical composition, so it is difficult to remove or eliminate them **(Hadi et al., 2019)**. Hence, it is necessary to find a good method of treating wastewater to avoid coloration of water systems **(Abed and Hussein, 2024)**. The ideal dye removal technique should be capable of removing large quantities of dyes from wastewater without causing secondary pollution, be cost-effective, and exhibit high efficiency **(Sen et al., 2012)**. Adsorption has been the most outstanding technique used to remove pollutants from the liquid phase onto an adsorbent surface because of its simple operation, cost-effectiveness, low energy consumption, lack of sludge generation, and insensitivity to highly toxic materials **(Alinejad-Mir et al., 2018)**. Dyes have been removed from wastewater using various adsorbents such as activated carbon, clay, silica, and porous materials **(Chen et al., 2018)**. However, there is growing interest in using biodegradable polymers to clean polluted water due to their high availability, low cost, ease of surface area, pore size distribution, and environmentally friendly nature **(Dassanayake et al., 2021; Abu Elella et al., 2024)**. Gelatin is one of the most valuable polymers extracted from the skin and bones of animals and has wide applications owing to significant biodegradability, biocompatibility, non-toxicity, and easy availability **(Mokrejš et al., 2019; Zhang et al., 2019)**. The network of gelatin is, however, intrinsically unstable; beyond the capacity of gel, it collapses and thus constrains its practical uses **(Cui et al., 2022)**. To improve the mechanical properties of the gelatin hydrogel, chemical crosslinking is frequently used (e.g., Glutaraldehyde) **(Li et al., 2021)**. Glutaraldehyde (GTA) is a commonly used crosslinking agent in the production of hydrogels due to its ability to stabilize biomaterials, its availability, and its cost-effectiveness **(Pal et al., 2009)**. This dialdehyde is very reactive with aldehydic groups, which have the potential of forming covalent bonds with other functional groups such as amines **(Sacks et al., 2007)**. Amino groups in gelatin crosslinked with the aldehyde groups of the GTA in the form of Schiff bases, which enhance the gelatin structure and its properties **(Wang et al., 2024).** It is worth mentioning that the inappropriate neutralization of GTA could lead to cytotoxicity **(Mugnaini et al., 2023)**. Although evaluating the crosslinking of gelatin with the help of dialdehydes has been explored in the context of improving mechanical strength, not enough research has been conducted to focus on the removal of Sunset Yellow using such a technique. Most of the existing literature focuses on commonly used dyes, thereby leaving a gap in the existing knowledge about the usefulness of glutaraldehyde-crosslinked gelatin against the complex structure of SY.

This study will explore the properties of crosslinked gelatin. The gelatin hydrogel that was produced was used in the adsorption of azo dyes in a water solution. It also investigates the

rate at which the dye adsorption process was affected by different parameters such as the concentration of dye, pH levels, and contact time. The structural behavior of the fabricated gelatin hydrogels was further analyzed using several physicochemical techniques, including SEM, FTIR, BET, EDX, TGA, and XRD. The thermodynamics and kinetics of the adsorption were also investigated. The research also aimed at exploring the gelatin hydrogel in terms of reuse and regeneration.

2. MATERIALS AND METHOD

2.1 Materials

Commercial gelatin (GE) (Type A, derived from bovine bones), along with glutaraldehyde (GTA; 25% for synthesis), hydrochloric acid (HCl), and ethanol (99% pure) were purchased from Arwa Medical (Baghdad, Iraq). Sunset yellow dye (SY) was supplied by Asalat Alhusam (Baghdad, Iraq).

2.2 Glutaraldehyde-Treated Gelatin

Type A gelatin was modified with GTA according to the method described by **(Michelini et al., 2020)**. The cross-linking process using GTA required dissolving 1.5 g of gelatin in 10 ml of water at a temperature of 50 degrees Celsius. While stirring continuously (about 500 RPM), 0.18 ml of GTA was quickly added. After 10 seconds, the resulting mixture was placed in Petri dishes and incubated for 24 hours at 40°C. The sample was then purified by immersion in ethanol for 24 hours, followed by deionized water for another 24 hours, which assisted in the removal of unreacted residues of GTA. Finally, the sample was dried by immersion in a 50% v/v ethanol solution for two hours, followed by immersion in a 100% ethanol solution for an additional two hours. The addition of ethanol in the last step was to help in the drying process. It was filtered then with filter paper and left to dry completely before use. **Fig.1** shows the modification process of gelatin with GTA.

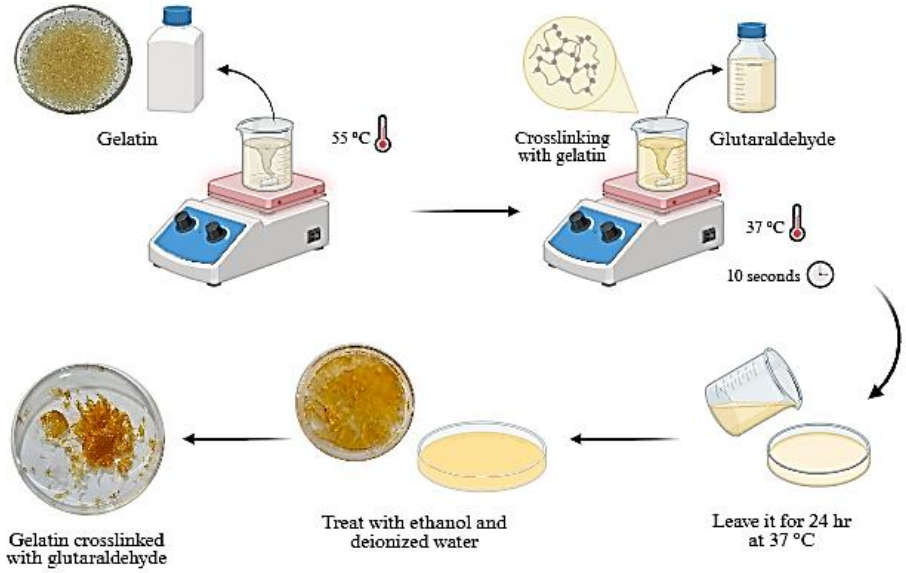

Figure 1. Method of producing glutaraldehyde-treated gelatin.

Gelatin has a unique amino acid sequence and a range of functional groups, which make it a good choice in developing chemical hydrogels in film form by reacting with small molecules that contain reactive functional groups, such as aldehyde groups. As mentioned above, it is generally known that the gelatin crosslinking mechanism by glutaraldehyde can be explained by the effect of the reaction between the aldehyde functional groups and non-protonated free amino groups (-NH_2) of gelatin in the form of Schiff bases as shown in **Fig. 2 (Farris et al., 2010a)**

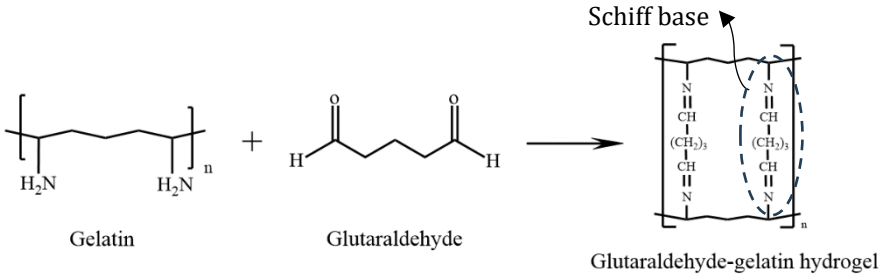

Figure 2. preparation of GTA-GE via Schiff bases.

2.3 Batch Adsorption Study

Sunset yellow dye (0.05 g) was dissolved in 1 liter of water to make a standard solution of this dye with a concentration of 50 mg/L. The absorbance was recorded under UV-Vis spectroscopy at different levels of dye (between 10 and 50 mg/L), as shown in **Fig. 3**. The initial standard solution was diluted to get these concentrations, as per the requirement of the titration curve and the adsorption process **(de Sá et al., 2013)**. It was found that the sunset yellow showed the highest absorption at 482 nm.

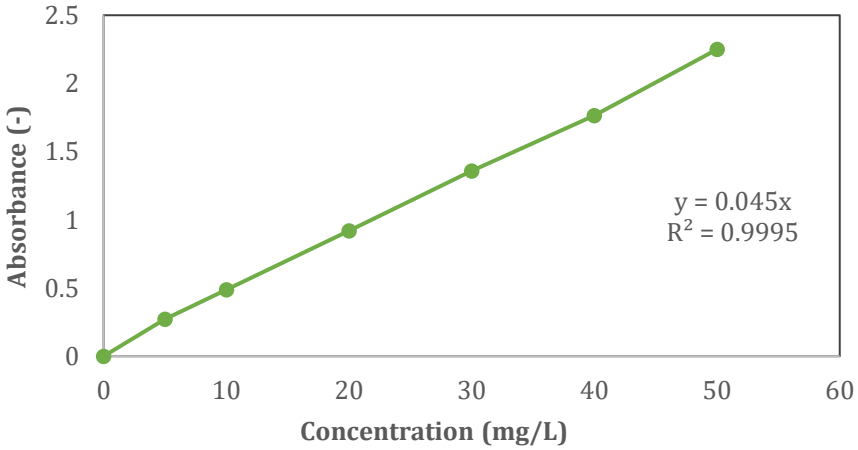

Figure 3. Calibration curve of sunset yellow dye.

The effect of initial concentration, contact time and dosage of adsorbent on the batch adsorption process was measured by adding various concentrations of sunset yellow dye (between 10 and 50 mg/L) under the same temperature and rate of agitation. Later on, a 0.1 M solution of HCl was added in a few drops until the pH level of the stock solution became 4, which was determined by using pH strips. In order to test the influence of contact time on dye adsorption, 0.1 g of gelatin was added to the stock solution. 4 mL samples of the stock solution were collected every 20 minutes and used in the analysis in the UV spectrometer to

measure the absorbance and ascertain the final concentrations. This was repeated until equilibrium was reached. The adsorption capacity q_t (mg/g), was calculated using Eq. (1)**(Piccin et al., 2012)**:

$$q_t = \left(\frac{C_i - C_t}{W}\right) \times V \quad (1)$$

Where C_i and C_t are the initial and at time t concentration of the dye (mg/L), respectively. W is the weight of the adsorbent material (g), and V represents the volume of the solution (L).

2.4 Mechanisms of SY Dye Adsorption

The adsorption of dye from contaminated water on the surface of an adsorbent is achieved via various adsorption mechanisms, as schematically shown in **Fig. 4**. As it has been noted, electrostatic forces, in addition to hydrogen bonds, could occur between the cationic segments of gelatin and the anionic parts of the SY dye **(Hu et al., 2006)**. Hydrogen bonding between the amine groups of the oxygen atoms of the dye molecules and the carbonyl groups of the crosslinked gelatin was expected **(Panić et al., 2013)**. Given the fact that the majority of the polymer materials and the azo dye have ionic properties, it is expected that the pH of the solution will also affect the structure of the dye as well as the polymeric material. Also, the changes in pH will tend to have a drastic effect on the surface modification of the adsorbents, as well as the degree of ionization of the functional groups present and the adsorption process **(Sun et al., 2010)**. When it is observed that the process of dye absorption is associated with the electrostatic attraction between the dye and the polymeric material, then at a certain level of pH, charged groups on the polymer chains would be made available to participate in the process of electrostatic interactions with the dye ions **(Panić et al., 2013)**.

Finally, van der Waals forces are atomically and molecularly based short-range forces that are significantly weaker compared to other driving forces **(Aoyama et al., 2022)**. Although the van der Waals forces can be present in the process of adsorption, they play a relatively insignificant role that is limited by comparison to the dominance of the electrostatic forces that predominantly control the adsorption of dye molecules.

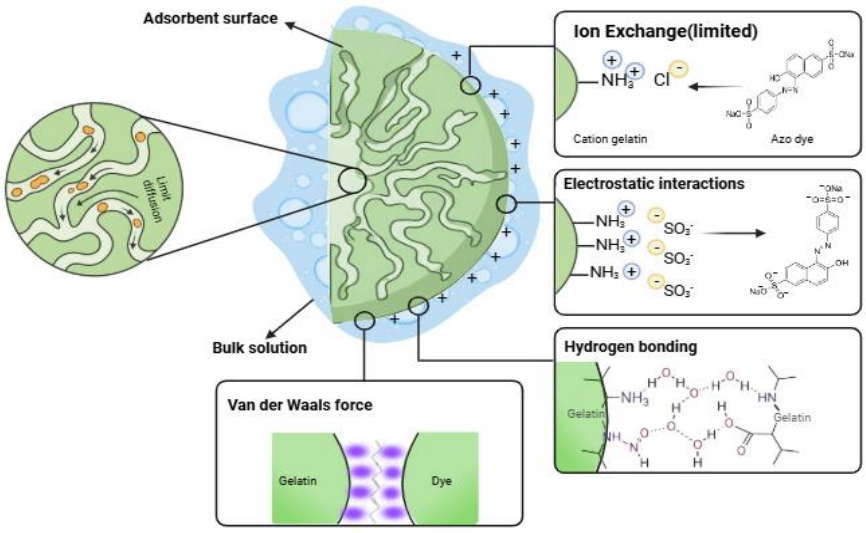

Figure 4. Mechanisms of Sunset Yellow dye adsorption.

3. RESULTS AND DISCUSSION

3.1 Characterization of the Commercial and Crosslinked Gelatin

3.1.1 Fourier Transform Infrared Analysis

Fourier transform infrared spectroscopy was used to analyze the functional groups present in GE and GTA-GE. This method is usually used to determine particular functional groups or chemical bonds in substances **(Balakrishnan et al., 2013)**. **Fig. 5** shows the FTIR spectra of both GE and GTA-GE. It can be noticed that, in the absence of a crosslinker, there is a shoulder-like peak at around 3236.55 cm^{-1} to denote a non-bonded -OH stretching band. In the recorded spectra, it can be seen that two additional bands are typical of gelatin and, more generally, protein matrices **(Farris et al., 2010b)**. In GE, the first band is observed in 1697.36, 1681.93, and 1649.14 cm^{-1}, whereas in GTA-GE, the band is denoted in 1637.56 and 1616.35 cm^{-1}; this is the amide I band, which is mainly associated with C=O stretching. The amide II band occurs at 1541.12 and 1516.05 cm^{-1}, which are the N=CH bending vibrations and C-N stretching vibrations in GE **(Chittur, 1998)**. A slight change in the amide II band of the gelatin cross-linked films is an indication that the amide groups may undergo cross-linking reactions to produce Schiff bases. Also, GE displays an amide III peak (C-N stretch and N-H in-phase bending) at 1195.87 cm^{-1}, CH_2 at 2949.16 cm^{-1}, and amide A at 3450 cm^{-1}; these are the characteristic features of gelatin **(Benjakul et al., 2009)**. Glutaraldehyde has an aldehyde group (-CHO) that reacts with the amino group. The uncrosslinked and crosslinked gelatin could be distinguished by a progressive color change of the sample from light yellow to orange **(Imani et al., 2013)**. Besides, another peak was observed at about 1540 cm^{-1}, due to the reaction of amide II in gelatin with the aldehyde groups in GTA **(Li et al., 2016)**.

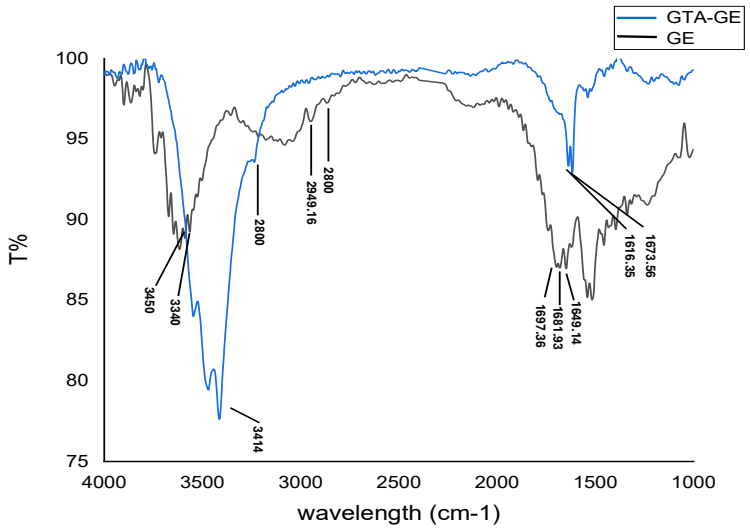

Figure 5. FTIR spectra of GE and GTA-GE.

3.1.2 X-ray Diffraction Analysis

Fig. 6 shows the XRD spectrum of GE and GTA-GE hydrogel composites. The XRD analysis has been used to identify the crystalline phase of the scaffolds in terms of the orientation of the diffraction peaks, their patterns, and the determination of the average crystalline size of GE and GTA-GE. There is a broad peak in both pure GE and GTA-GE at 2θ= 20.1°. The results of this analysis show that the presence of gelatin inhibits the crystallization process in

crosslinked and non-crosslinked gelatin hydrogels, and due to this, the amorphous nature of GE and GTA-GE can be noticed in this figure **(EL-Sayed et al., 2017)**

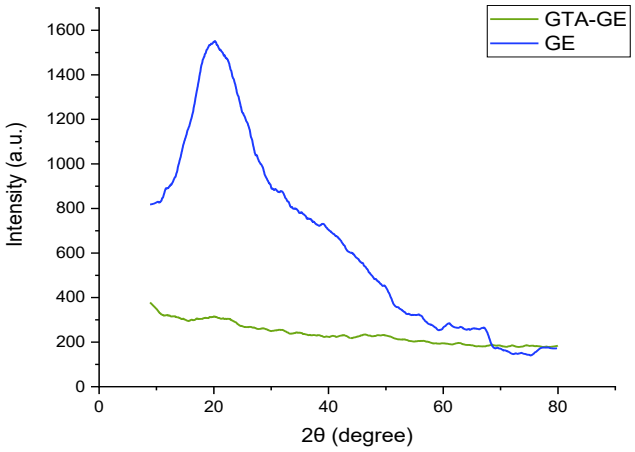

Figure 6. XRD spectra of GE and GTA-GE.

3.1.3 Scanning Electron Microscopy and Energy-Dispersive X-Ray Analysis

The SEM images and EDX spectrum of GE and GTA-GE are displayed in **Fig. 7**. SEM analysis was used to investigate the morphologies and structures of gelatin adsorbents. In this study, SEM was used to consider the differences between the gelatin structure before and after crosslinking.

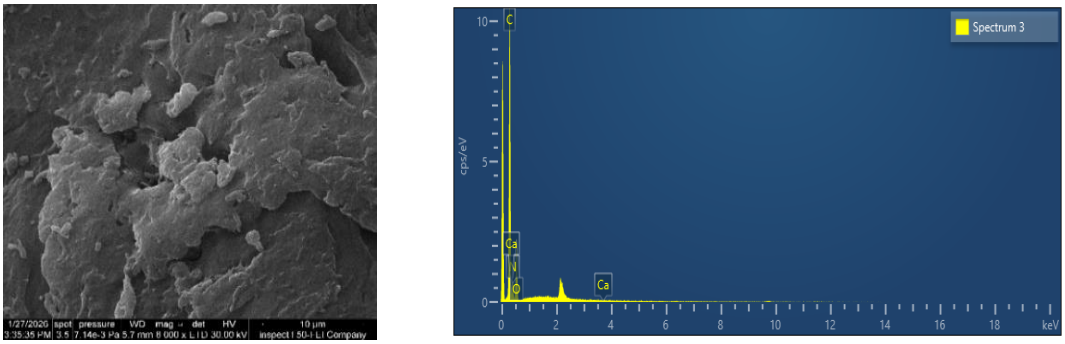

(a)

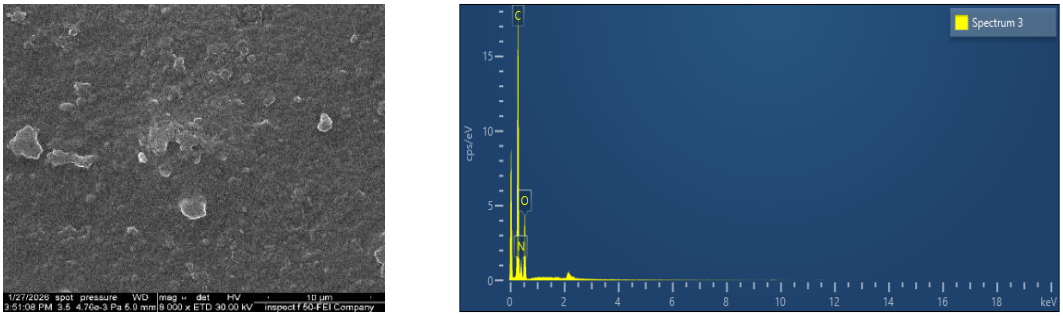

(b)

Figure 7. SEM with EDX of (a) Gelatin (b) Gelatin with glutaraldehyde.

The surface of the unmodified GE was rough and fractured as compared to the crosslinked GE film, which had a polished and compact surface owing to the addition of GTA **(Maroufi et al., 2022)**. Studying the gelatin films that were crosslinked with glutaraldehyde and then

oriented by force, found that the alignment of the gelatin chains became better in the direction of the applied force. What we also found is that the thickness of the layers and the gap between them shrank due to orientation by treatment **(De Carvalho and Grosso, 2004)**. In addition, an energy dispersive X-ray (EDX) analysis was performed to assess the composition in terms of elements in the hydrogels. The EDX spectrum showed the element composition of GE (consisting of C, N, and O) and GTA-GE (consisting of O, C, and N) with some traces of Ca. **(Masri et al., 2022)**

3.1.4 Brunauer–Emmett–Teller analysis

The nitrogen adsorption–desorption isotherms of GE and GTA-GE are shown in **Fig. 8**. The displayed materials all had Type IV adsorption isotherms, which means that they have mesopores. The fact that there is a hysteresis loop at the P/Po values of approximately 0.8 to 1.0 indicates that the structural regularity is low **(Ulfa et al., 2022)**. The surface area of the BET for GE is 4.559 m^2/g and 22.603 m^2/g for GTA-GE. GE had a smaller surface area than that of GTA-GE. This is given the fact that the aldehyde group is present, and it results in the formation of Schiff bases in the pores and on the outer surface of GTA-GE **(Prashanna Suvaitha and Venkatachalam, 2023).** This effect is related to the role of crosslinking in strengthening the protein network, which helps retain nanoscale gaps between the crosslinked chains. These findings suggest that the crosslinking process not only enhances the mechanical stability of the gelatin matrix but also has a positive effect on the adsorption process.

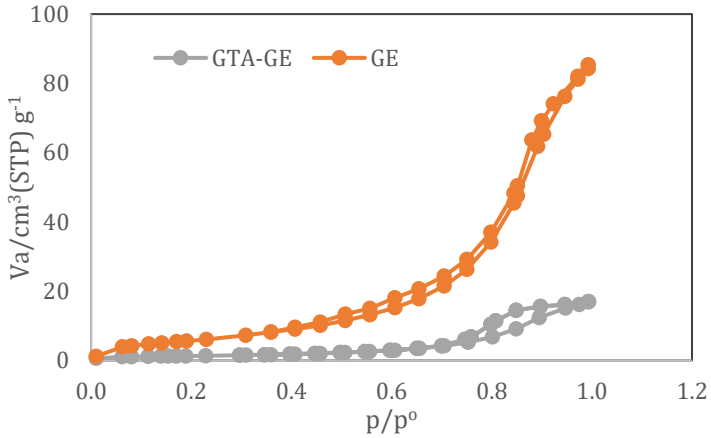

Figure 8. The N_2 adsorption–desorption isotherms of GE and GTA-GE.

3.1.5 Thermogravimetric Analysis

The TGA analysis of GE and GTA-GE is presented in **Fig. 9**. To determine the thermal stability of gelatin microspheres, the thermogravimetric analysis was used. These results revealed that GE and GTA-GE samples had multistep decomposition. This habit can be attributed to various causes, such as moisture loss, decomposition of amino acid fragments, and damage to the polymer matrix. Also, the data obtained indicated that thermal decomposition in GTA-GE sample required a higher temperature than in GE sample, meaning that gelatin chemical modification with GTA can significantly increase the thermal stability of the substance **(Zhu et al., 2019)**. The evaporation of moisture and volatile substances can explain the first weight loss, but the subsequent decrease is related to the polymeric structure degradation. The GTA-GE was also found to lose weight (17%), due to the loss of the absorbed moisture and volatile compounds in the temperature range of 30-150°C. This was followed by weight

loss of 35.6 and 21.7 % at 150-330°C and 330-550°C, respectively. Conversely, GE exhibited a primary weight loss ratio of about 13.8 % as it was heated between 25-200°C as a result of moisture evaporation, and then a second and third weight loss ratio of about 47.4 and 31.2 %, respectively, at temperatures 200-450°C and 450-850°C. Thermograms show that GE started decomposing at 230°C and GTA-GE started degrading at 280°C, which proves that GTA-GE is more thermally stable than GE **(Sethi et al., 2020)**. This enhanced structural stability ensures the integrity of GTA-GE during the adsorption process and makes it possible to reuse it in a number of adsorption cycles.

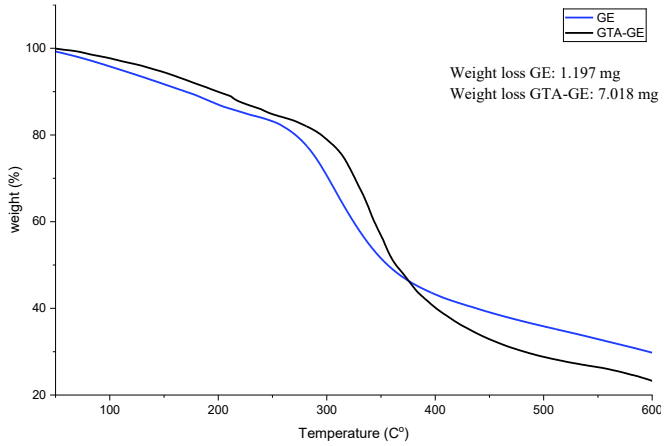

Figure 9. The TGA curves of GE and GTA-GE.

3.2 Effect of Initial Dye Concentration on Adsorption

Fig. 10 shows the effect of the initial concentration of SY in solutions on the rate of adsorption of crosslinked and un-crosslinked gelatin. The experiments have been run with a constant dosage of adsorbent of 0.1 g/ 50 ml of solution, at a room temperature, pH of 4 at initial SY concentrations of (10-50 mg/L) and different time intervals. Results are shown in **Table 1**. It is evident that the percentage of adsorption efficiency of glutaraldehyde treated and untreated gelatin medium decreased with an increase in the initial concentration of dye. It is important to note that it took 80 minutes before equilibrium was achieved with glutaraldehyde treated gelatin. The delay can be explained by the fact that it has macro and micro pores in GTA-GE that increase the time of interaction between the dye molecules and the adsorbent material .The next process is diffusion into the porous structure of the adsorbent itself, which requires a long contact time **(Garg et al., 2004)**.

During the process of dye adsorption, the dye molecules must first interact with the boundary layer effect. Then they have to be diffused out of this boundary layer film to the surface of the adsorbent, and lastly, they are diffused into the porous structure of the adsorbent **(Lata et al., 2007)**. This process takes place because the dye molecules are attracted to the adsorbent by attractive forces such as Van der Waals' forces and electrostatic forces. The rapid diffusion to the external surface is followed by a rapid diffusion into the intraparticle matrix, and the equilibrium is reached in 80 minutes **(Abd El-Latif et al., 2010)**. The rate of adsorption at this stage is associated with the realization of saturation equilibrium of the adsorbent. **(Kalash et al., 2020)**.

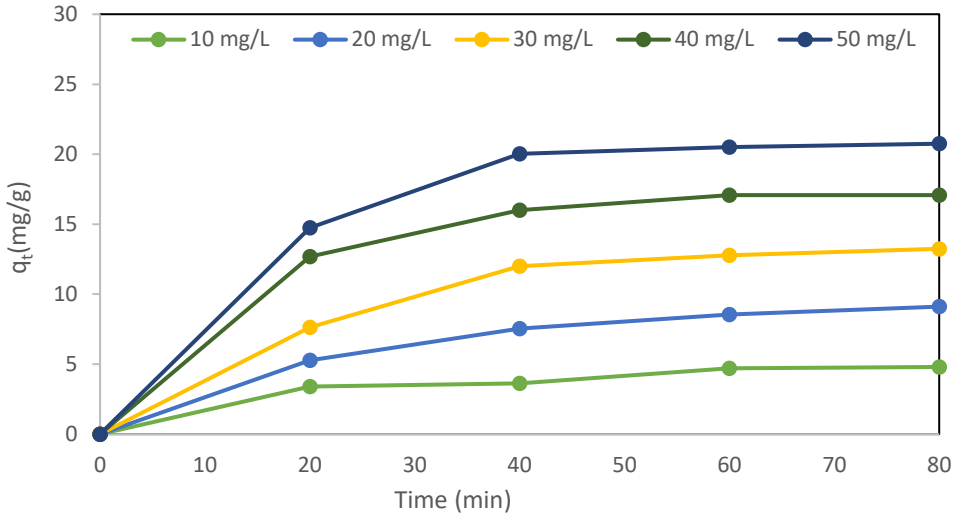

(a)

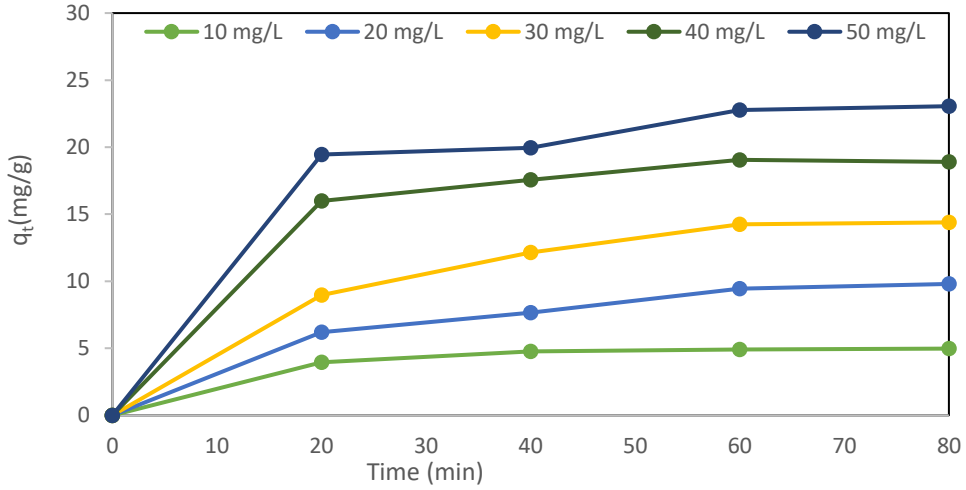

(b)

Figure 10. Initial SY concentration and contact time's effect on the adsorption process of: (a) GE and (b) GTA-GE.

Table 1. Effect of sunset yellow concentration on the dye adsorption

Initial dye concentration (mg/L)	Dye removal % at 80 min		Adsorption capacity(mg/g)	
	GTA-GE	GE	GTA-GE	GE
10	99.778	96.000	4.978	4.8
20	99.667	91.111	9.800	9.111
30	98.222	88.148	14.389	13.244
40	95.000	85.333	18.911	18.144
50	88.444	83.000	23.056	21.333

Fig. 11 shows the relationship that exists between the concentration of SY dye and rate of removal as well as adsorption capacity. It was noted that q_e increased with increase in concentration of this dye from 4.978 to 23.056 mg/g for GTA-GE and 4.8 to 21.333 mg/g for GE. A higher initial concentration of the dye is a major driving force that can be used in reducing the resistance associated with mass transfer of the liquid solution and with the

solid phase of a certain quantity of adsorbent. On the other hand, the percentage of SY dye removal decreased from 88.4 % to 99.8 % with GTA-GE and at 83 % to 96 % with GE as the initial concentration of SY dye was increased to 10 mg/L up to 50 mg/L**(Dawood et al., 2016).**

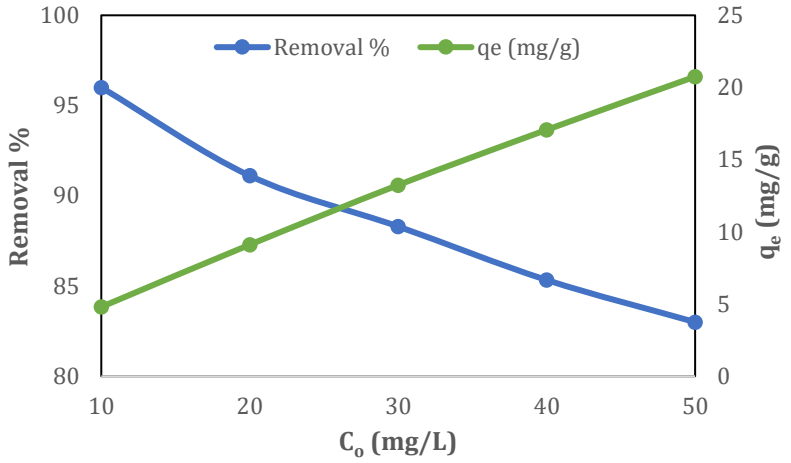

(a)

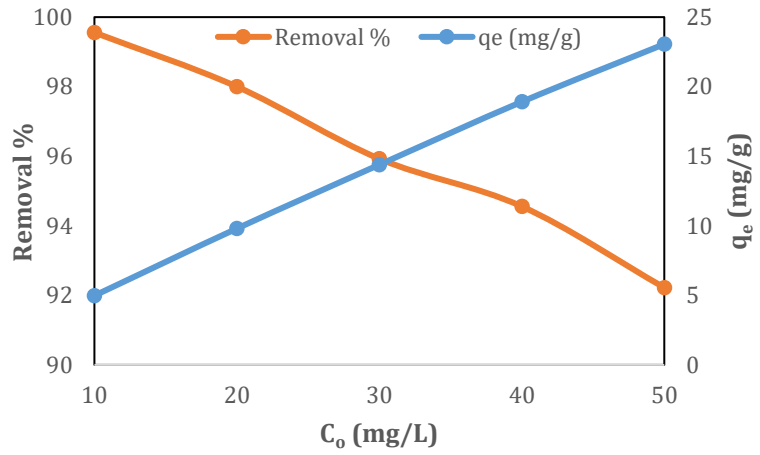

(b)

Figure 11. Effect of initial dye concentration(mg/L) on the removal% and qe(mg/g) for (a) GE and (b) GTA-GE.

3.3 Effect of Adsorbent Dose

The experiment investigated the adsorption of SY to the glutaraldehyde-treated and untreated gelatin by adjusting the quantity of the adsorbent (0.05 to 0.25 g/50 ml) in the test solution and maintaining the constant variables: initial dye concentration (30 mg/L), at room temperature, contact time (80 min), and pH (4). **Fig. 12** shows the effect of dosage on the adsorption process. The findings indicated that in the case of GTA-GE, adsorption at the equilibrium time (80 min) increased from 80.2 to 99.9 % with a rise in the adsorbent dosage. Contrarily, in untreated gelatin, the percentage adsorption increased from 75.1 to 98.2 % with the increase in the quantity of the adsorbent from 0.05 to 0.25 g/50 ml. The increase in adsorption when the dosage of adsorbent is increased could be explained by the increased surface area and the presence of more adsorption sites **(Abdullah et al., 2005)**. On the other hand, the fact that the adsorption capacity (qe) decreases with the increase in adsorbent dosage is possibly because the particles that make up an adsorbent interact with each other

(with aggregation and agglomeration processes being the main ones), and the total surface area is lowered**(Shakoor and Nasar, 2016)**. This is because a fixed amount of gelatin can only be able to take a certain amount of dye. Therefore, the more adsorbent we have, the more dye can be purified by a given mass of gelatin. This decrease in qe (mg/g) as the mass of the adsorbent increases is attributed to the separation in flux or the concentration gradient between the solute concentration in the solution and the concentration on the surface of the adsorbent. Thus, the mass of adsorbent and the mass of adsorbed dye per unit weight of adsorbent become smaller, and the qe value decreases with the increase in the concentration of adsorbent mass **(Vadivelan and Vasanth Kumar, 2005)**

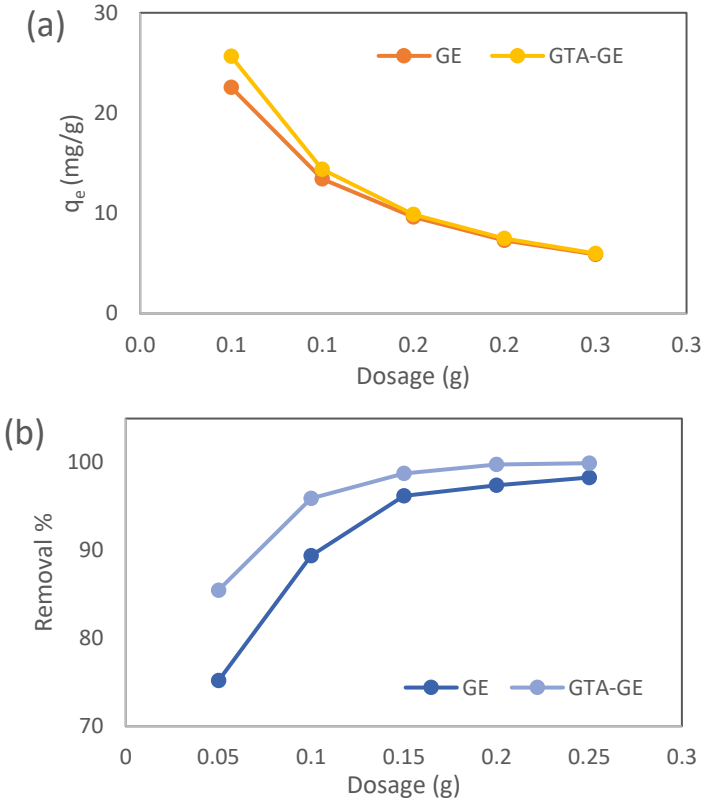

Figure 12. Effect of adsorbent dose on : (a) qe and (b) removal rate for GE and GTA-GE.

3.4 Effect of pH

The preliminary pH effect on the adsorption process was analyzed by performing a batch adsorption experiment with pH of 2, 4, 5, 6, and 8. The values showed that in the case of GTA-GE adsorption, the capacity was above 14.7 mg/g in the pH range of 2 to 4, as shown in **Fig. 13**. The best level of pH was found to be 4. In such circumstances, 100mg mass dosage with an initial concentration of 30mg/L produced an equilibrium adsorption capacity of 14.733 mg/g. For GE, the capacity was above 13 in the pH range (2-4), and the maximum capacity was achieved when pH equalled four **(Abu-Nada et al., 2021)**. By lowering pH value, the -NH_2 groups on the surface of GTA-GE and GE became more protonated, leading to a positive charge, which allowed the positively charged adsorbent surface to interact with the

negatively charged SY molecules. The higher the values of pH, the lower the protonation and the surface of the adsorbent became more negatively charged **(Yinghua et al., 2021)**

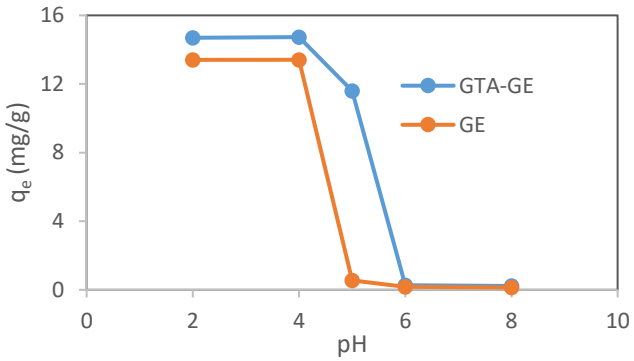

Figure 13. Effect of pH on the capacity for GE and GTA-GE. concentration: 30 mg/L, volume: 50 mL, temperature: 25 °C, adsorbent dosage:100 mg.

3.5 Adsorption Kinetics

The research about adsorption processes was devoted to the principles of mass transfer and chemical reactions, which were discussed on the basis of experimental data along with the help of kinetic equations, including the pseudo-first order and pseudo-second order models. The pseudo-first order kinetic model is mathematically expressed as a linear Eq. (2):

$$log(q_e - q_t) = log\, q_e - (K_1/2.303)t \quad (2)$$

in which the functions of q_t (mg·g^{-1}) and t (min^{-1}) are the adsorption capacity at time t and K_1 (min^{-1}) is the rate constant for pseudo-first-order adsorption, and qe is the adsorption capacity at equilibrium. The results of this kinetic study are shown in **Fig. 14**.

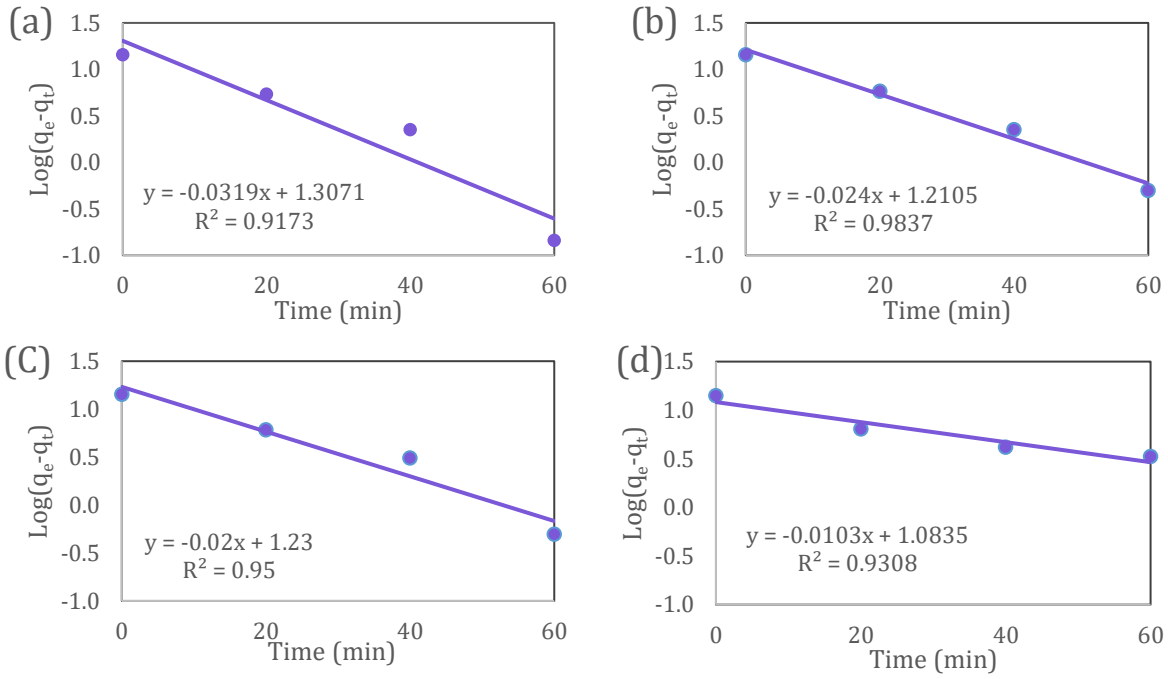

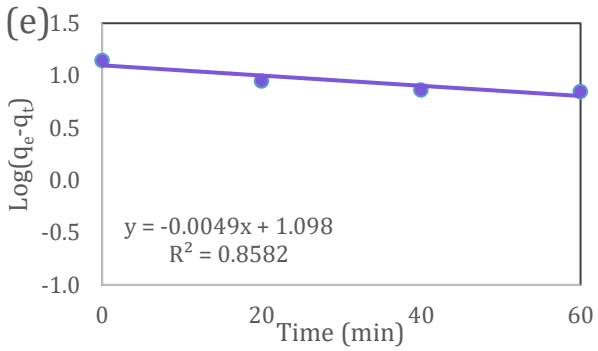

Figure 14. pseudo-first order kinetics of SY adsorption on GTA-GE at :(a) 298K, (b) 308K, (c) 318K, (d) 328K, and (e) 338K (Conc. = 30 mg/L, V = 50 mL, pH 4).

The pseudo-second order kinetic model in linear form is as Eq. (3):

$$\frac{t}{q_t} = \frac{1}{K_2 q_e^2} + \left(\frac{1}{q_e}\right) t \tag{3}$$

where K_2 ($g \cdot mg^{-1} \cdot min^{-1}$) is the rate constant of the pseudo-second order adsorption. **Fig. 15** shows the result of pseudo-first order kinetic

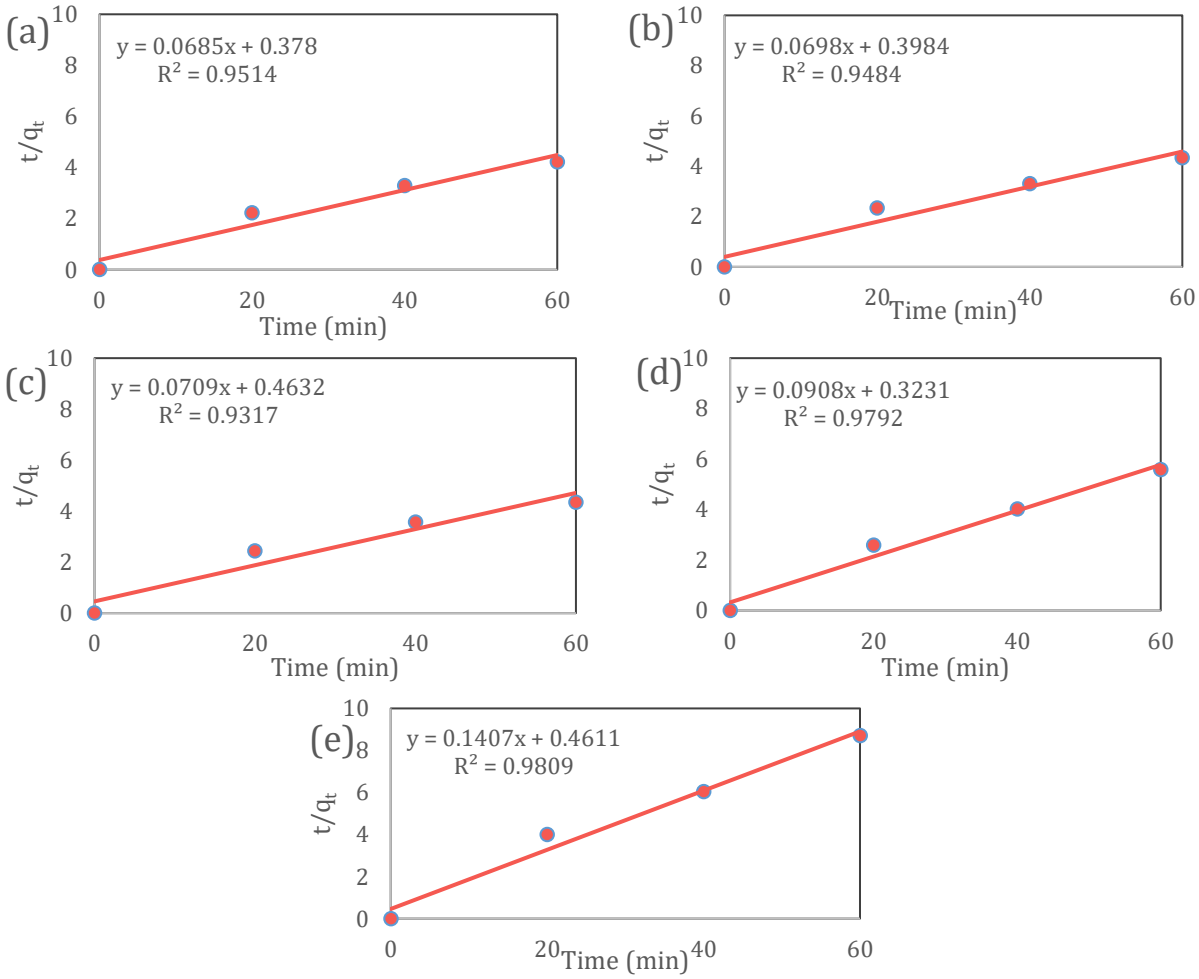

Figure 15. pseudo-second order kinetic of SY adsorption on GTA-GE at :(a) 298K, (b) 308K, (c) 318K, (d) 328K, and (e) 338K (Conc. = 30 mg/L, V = 50 mL, pH 4).

Table 2 shows that the pseudo-second order kinetic model is more accurate in displaying the kinetics of adsorption system compared to the pseudo-first order model, depending on the value of R^2. The pseudo-second order model has a correlation coefficient (R^2=0.981) of the GTA-GE adsorbent. This implies that adsorption of SY has occurred via chemisorption, which involves the development of covalent bonds and exchange of ions between the adsorbent and the adsorbate **(Aragaw, 2020)**.

Table 2. Adsorption kinetics of SY dye on GTA-GE.

T/K	Pseudo First order			Pseudo-Second order		
	R^2	K_1 (min^{-1})	q_e (mg/g)	R^2	K_2 ($g \cdot mg^{-1} \cdot min^{-1}$)	q_e (mg/g)
298	0.917	0.073	20.281	0.951	0.012	14.599
308	0.984	0.055	16.238	0.942	0.012	14.327
318	0.945	0.054	17.069	0.932	0.011	14.104
328	0.931	0.024	12.12	0.977	0.026	11.013
338	0.858	0.011	12.531	0.981	0.043	7.107

3.6 Adsorption Isotherm

Fig. 16 illustrates the relationship existing between the concentration of the dye and the adsorption capacity at equilibrium. Adsorption of SY occurred very quickly within a few minutes, and then the rate started decreasing slowly. When a single layer of saturated solute molecules covers the surface of the adsorbent, maximum adsorption is attained. In such circumstances, no adsorbate molecules move over the adsorbent surface, and the adsorption energy is maintained constantly, which follows the theoretical Langmuir sorption isotherm **(Filice et al., 2021)**.
The Langmuir isotherm is depicted in Eq. (4).

$$\frac{C_e}{q_e} = \frac{1}{K_L . q_{max}} + \frac{C_e}{q_{max}} \tag{4}$$

Where q_{max}(mg/g) and K_L(L/mg) are Langmuir constants. q_{max} represent the maximum adsorption capacity, while $K_L$represent the energy adsorption constant, and C_e (mg/L) represent the concentration of dye at equilibrium. q_{max} and K_L were obtained from the slope and intercepts shown in **Fig. 17**.

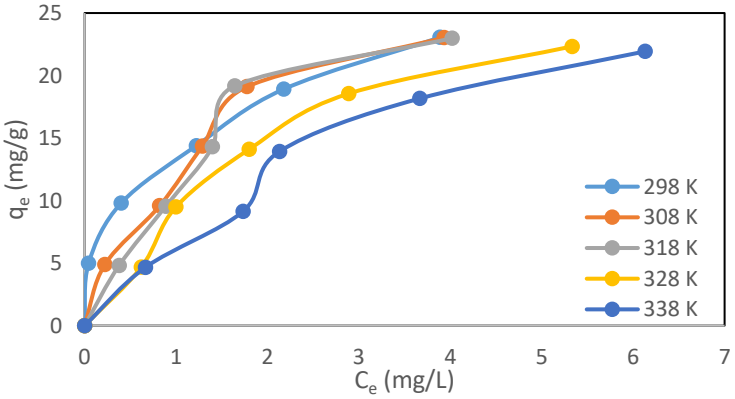

Figure 16. Adsorption isotherm of SY on GTA-GE at different temperatures.

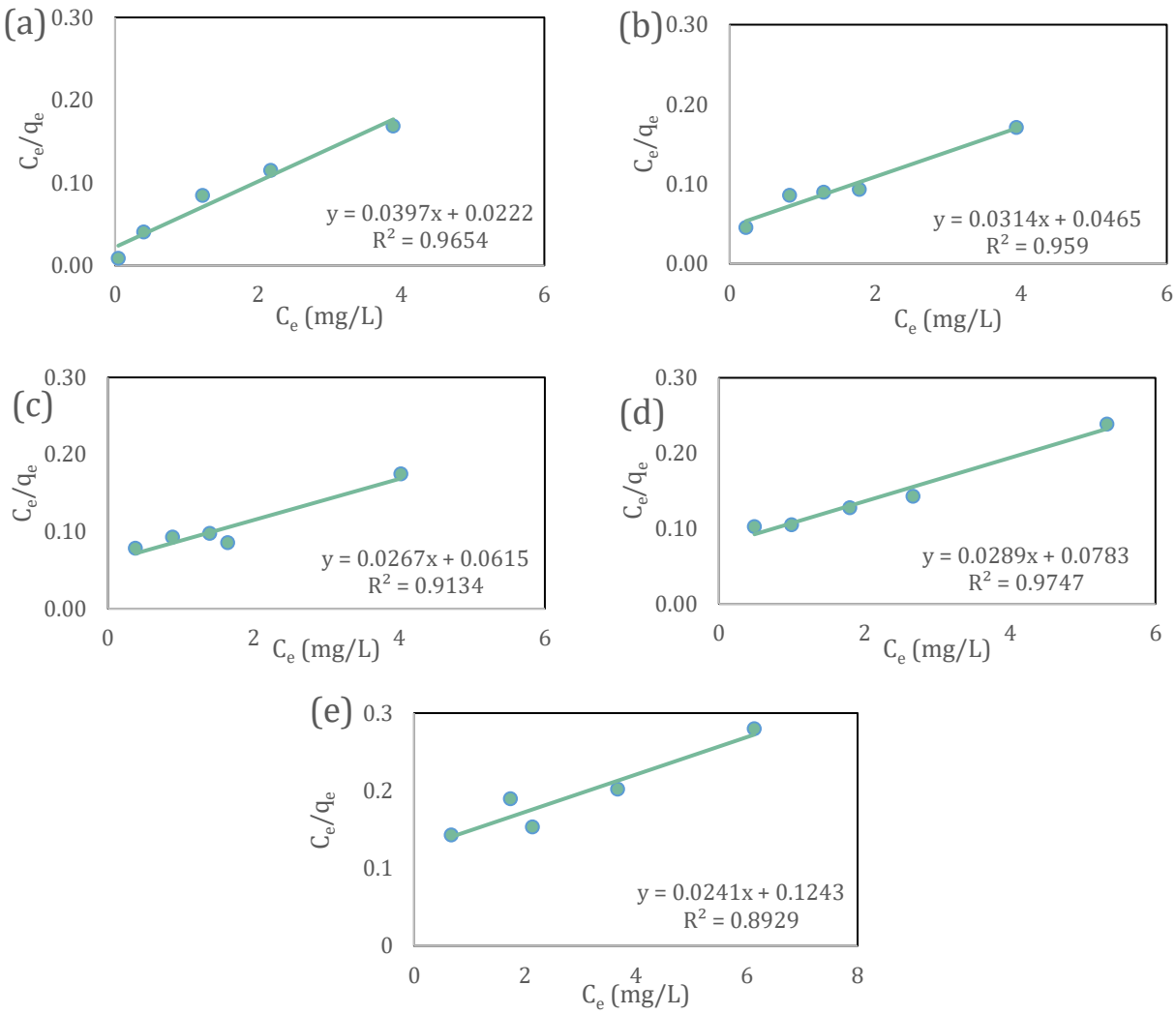

Figure 17. Langmuir linear form of SY adsorption on GTA-GE at :(a) 298K, (b) 308K, (c) 318K, (d) 328K, and (e) 338K (C_o= 10-50 mg/L, V = 50 mL, pH 4).

Eq. (5) also may be used to determine whether the adsorption process follows the Freundlich isotherm and to estimate its constants, just as the Langmuir adsorption isotherm. In case the observed results of the experiment demonstrate great linearity with this equation, it is possible to conclude that the adsorption process can comply with the Freundlich adsorption isotherm **(Chung et al., 2015)**

$$ln\, q_e = ln\, K_f + \frac{1}{n} ln\, C_e \quad (5)$$

In which K_f is the capacity of adsorption related to the Freundlich constant (mg/L), and n is a dimensionless constant **(Hashemian et al., 2013)**. **Fig. 18** illustrates how the values of n and K_f were calculated from the slope and intercept of the fitted line. Based on R^2 values (regression coefficients) in **Table 3**, the Freundlich model is suitable to describe a heterogeneous coverage of SY on GTA-GE particles and the adsorption interaction

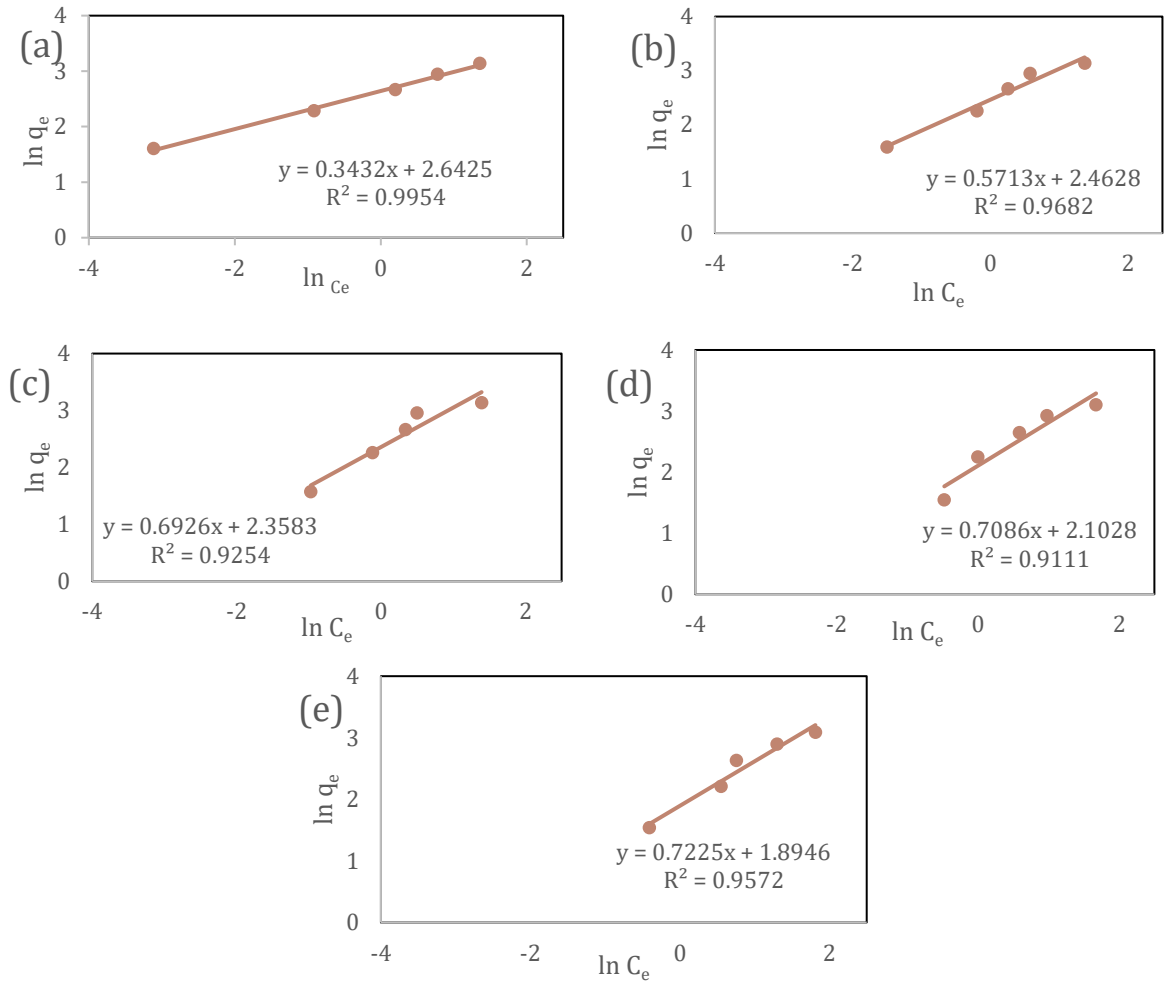

Figure 18. Freundlich linear form of SY adsorption on GTA-GE at :(a) 298K, (b) 308K, (c) 318K, (d) 328K, and (e) 338K (C_o= 10-50 mg/L, V = 50 mL, pH 4).

Moreover, this model gives a true approximation of the maximum SY adsorption capacity of the GTA-GE at 298 K (R^2 = 0.995) **(El-Azazy et al., 2019)**. According to the coefficients calculated using the Sips isotherm model, parameter n is greater than one, meaning that there is some extent of heterogeneity in this system **(Shahryari et al., 2010)**.

Table 3. Adsorption isotherm parameters of SY dye on GTA-GE.

T/K	Langmuir model			Freundlich model		
	R^2	qmax (mg/g)	K_L(L/mg)	R^2	K_f(L/mg)	n
298	0.965	25.189	1.788	0.995	14.048	2.914
308	0.959	31.847	0.675	0.968	11.737	1.75
318	0.913	37.453	0.434	0.925	10.572	1.443
328	0.977	34.602	0.369	0.911	8.189	1.411
338	0.893	41.493	0.194	0.957	6.649	1.384

3.7 Thermodynamic Study

Changes in Gibbs free energy (ΔG), entropy (ΔS), and enthalpy (ΔH) are important thermodynamic variables to analyze the adsorption process. These values were calculated by employing Eqs. (6) and (7) at five different temperatures and the results were shown in

Table 4. ΔH and ΔS were calculated from the van't Hoff plot between $\ln K_c$ vs. 1/T as shown in **Fig. 19**.

$$\Delta G = -RT\, ln\, K_c \quad (6)$$

$$lnK_c = \frac{\Delta S}{R} - \frac{\Delta H}{RT} \quad (7)$$

Where T (K) is the absolute temperature, R (8.314J/mol. k) is the universal constant, and K_c is the equilibrium constant. **(Aragaw and Alene, 2022)**

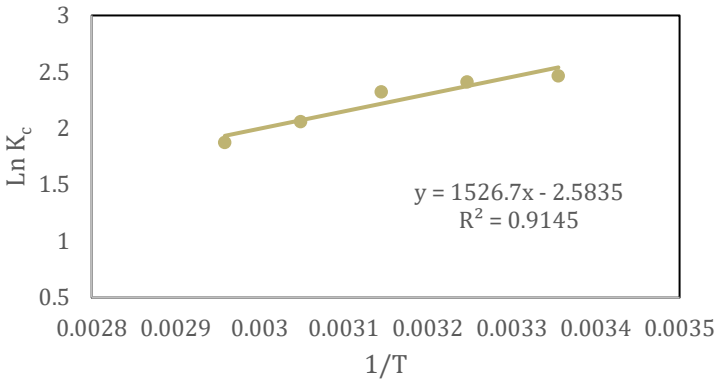

Figure 19. Van't Hoff plots of adsorption SY on GTA-GE.

Table 4 estimates the parameters at various temperatures. Negative value of the ΔH of -12.693kJ/mol indicates that the process of adsorption is exothermic and that the van der Waals force is also a major factor in physisorption. Moreover, negative values of ΔG prove that the adsorption of SY is thermodynamically favorable and spontaneous. However, when the temperature increases, the adsorption process becomes nonspontaneous, and the efficiency of dye adsorption decreases. On the same note, the negative value of ΔS (-0.021 mol. k) shows that at the interface of the solid solution, the degree of randomness decreases due to the adsorption of SY on GTA-GE **(Fatombi et al., 2019)**

Table 4. The thermodynamic properties of SY adsorption.

T/K	ΔG(kJ/mol)	ΔH(kJ/mol)	ΔS (kJ/mole.K)
298	-6.11	-12.693	-0.021
308	-6.172		
318	-6.144		
328	-5.613		
338	-5.273		

3.8 Desorption Study

The importance of desorption is brought by different reasons among them being the ability to explain the process of adsorption, the ability to reuse adsorbents and reduction of secondary wastes. In the desorption experiments, the raw GTA-GE adsorbent that was used earlier to adsorb SY dye solution was washed into the solution by the addition of 0.1 N NaOH and mixing the two in two hours. It was followed by drying the adsorbent to be used again **(Ramalakshmi et al., 2011)**. The dye removal and adsorption capacity reduced to 75.9% and 11.4 mg/g in the fourth run compared to the first run with 95.9% and 14.4 mg/g. Such a

progressive decrease observed throughout the regeneration cycles can be explained by the inaccessibility of some reactive sites after dye desorption or by inadequate removal of dyes within the adsorbent pores **(Kakavandi et al., 2019)**.
Consequently, the process of desorption investigation using NaOH implies that adsorption of SY dye on GTA-GE occurs mainly via ion exchange, accompanied by physical and chemisorption interactions **(Afroze et al., 2016)**. The observed decrease in the adsorption capacity with almost consecutive cycles is in line with previous studies on biopolymers **(Fatombi et al., 2019; Li et al., 2018)**, which show that structural integrity is normally maintained in the first few cycles, but degradation increases at cycle four and above. In addition, the shape of the GTA-GE was still the same after the fourth cycle due to the highly cross-linked three-dimensional network structure that is mechanically stable. As a result, it seems that the GTA-GE can be used as a good and recyclable adsorbent in industries **(Ren et al., 2021)**. **Fig. 20** represents a plot of removal efficiency, adsorption capacity, and number of cycles.

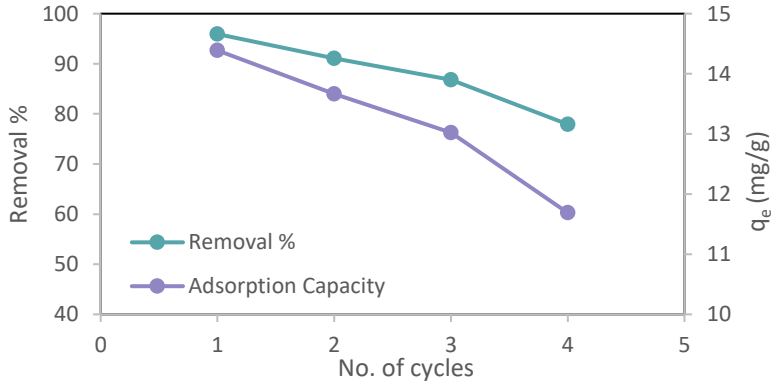

Figure 20. The plot of removal efficiency, adsorption capacity and number of cycles at concentration: 30 mg/L, volume: 50 mL, temperature: 25 °C, GTA-GE dosage:100 mg.

3.9 Comparison of SY Dye Adsorption on Different Adsorbents

Depending on the efficiency of the adsorbents in removing SY dye, as has been shown in **Table 5**, GTA-GE proved to be more efficient than the other materials. It follows that GTA-GE has potential as a useful adsorbent in the removal of dye in aqueous solutions.

Table 5. Comparison of removal% with various adsorbents for SY dye adsorption.

Adsorbents	Removal %	References
SBA-15/Pr-Im	74.9-91	**(Prashanna Suvaitha and Venkatachalam, 2023)**
Alligator weed activated carbon	50-90	**(Kong et al., 2017)**
Clay/Starch/$MnFe_2O_4$	72-95	**(Esvandi et al., 2020)**
Rhizopus arrhizus biomass	82-90	**(Salvi and Chattopadhyay, 2017)**
Fe_3O_4 nanoparticles	20-92	**(Takdastan et al., 2020)**
Gelatin modified with glutaraldehyde	88.4-99.7	Present Work

4. CONCLUSIONS

Gelatin is a feasible alternative to produce adsorbents that can be used in the wastewater treatment process due to its characteristics. The further benefits of using glutaraldehyde is to make gelatin more resistant to degradation and increase its mechanical strength. The performance of adsorptive removals of SY dye with GTA-GE and GE as the adsorbent was evaluated in this study. The efficiencies obtained were 99.8% and 96% in the removal of SY to GTA-GE and GE, respectively, under the optimum conditions, which were a dosage of the adsorbent of 0.1 g/50 mL, pH of 4, a contact time of 80 minutes and initial dye concentration ranging between 10 and 50 mg/L. For the adsorption kinetics, Pseudo-second order (R^2 = 0.981) provided the best fit. It means that covalent bonds and ion exchanges exist between the adsorbent and the adsorbate. Furthermore, the Freundlich isotherm (R^2 = 0.995) provided the best description of the adsorption isotherm data, showing a heterogeneous coverage of SY on GTA-GE particles. Also, a thermodynamic examination showed that dye adsorption onto GTA-GE is described as an exothermic (ΔH= -12.693kJ/mol), spontaneous process (ΔG < 0), and the degree of randomness decreases (ΔS =-0.021 mol. K). Regenerated adsorbent proved to be reusable four times with a significant drop in removal efficiency (~ from 95 to 70%), which means that it can be recycled and is stable. Even though GTA is costly, it is a single investment because the product can be recycled and used again. Altogether, the current research indicates that the discussed method is potentially practicable regarding adsorbent modification and successfully removes SY from water.

NOMENCLATURE

Symbol	Description	Symbol	Description
BET	Brunauer–Emmett–Teller	GE	gelatin
C_e	concentration at equilibrium	GTA-GE	gelatin crosslinked with glutaraldehyde
C_o	initial concentration of the dye (mg/L)	K_c	the equilibrium constant (L/g)
C_t	concentration of the dye at time t (mg/L)	K_f	the Freundlich constant (mg/L)
EDX	Energy-dispersive X-ray	K_L	the Langmuir constant
FTIR	Fourier transform infrared	K_1	the rate constant of pseudo-first order kinetics (min^{-1})
K_2	the rate constant of pseudo-second order ($g{\cdot}mg^{-1}{\cdot}min^{-1}$)	T	temperature (K)
n	degree of nonlinearity between adsorption process and the concentration of dye	t	time (min)
q_e	adsorption capacity at equilibrium (mg/g)	TGA	Thermogravimetric
q_t	the amount of adsorbed on the surface of gelatin at any time	V	the volume of the solution (L)
q_{max}	maximum adsorption capacity	W	the weight of the adsorbent material (g)
R	the gas constant in (J/mol. k)	XRD	X-ray diffraction
R^2	correlation coefficient	ΔG	standard free energy change (kJ/mol)
SEM	Scanning electron microscopy	ΔH	standard enthalpy change (kJ/mol)
SY	sunset yellow	ΔS	standard entropy change (kJ/mole.K)

Credit Authorship Contribution Statement

Haya M. Zobeer: Conceptualization, Methodology, Numerical modeling, Data analysis, writingoriginal draft, editing. Mahmmod Al- Mashhadani: Methodology, Writing review & editing, Supervision. Sanaa Al-sahib: Writing review & editing, Validation.

Declaration of Competing Interest

The authors declare that they have no known competing financial interests or personal relationships that could have appeared to influence the work reported in this paper.

REFERENCES

Abd El-Latif, M.M., Ibrahim, A.M. and El-Kady, M.F., 2010. Adsorption equilibrium, kinetics and thermodynamics of methylene blue from aqueous solutions using biopolymer oak sawdust composite. *Journal of American Science*, 6(6). https://doi.org/10.1016/j.egypro.2013.07.103.

Abdullah, A.L., Salleh, M.M., Siti Mazlina, M.K., Mazlina, M.S., Noor, M.J.M.M., Osman, M.R., Wagiran, R. and Sobri, S., 2005. Azo dye removal by adsorption using waste biomass: sugarcane bagasse. *International Journal of Engineering and Technology*, 2(1), pp. 8–13.

Abed, I.A. and Hussein, B.I., 2024. Effects of preparation conditions on performance of PES:PEG flat sheet membrane for MG dye separation. *Journal of Engineering*, 30(12), pp. 189–205. https://doi.org/10.31026/j.eng.2024.12.12.

Abu Elella, M.H., Aamer, N., Abdallah, H.M., López-Maldonado, E.A., Mohamed, Y.M.A., El Nazer, H.A. and Mohamed, R.R., 2024. Novel high-efficient adsorbent based on modified gelatin/montmorillonite nanocomposite for removal of malachite green dye. *Scientific Reports*, 14(1). https://doi.org/10.1038/s41598-024-51321-2.

Abu-Nada, A., Abdala, A. and McKay, G., 2021. Isotherm and kinetic modeling of strontium adsorption on graphene oxide. *Nanomaterials*, 11(11). https://doi.org/10.3390/nano11112780.

Afroze, S., Sen, T.K., Ang, M. and Nishioka, H., 2016. Adsorption of methylene blue dye from aqueous solution by novel biomass Eucalyptus sheathiana bark: equilibrium, kinetics, thermodynamics and mechanism. *Desalination and Water Treatment*, 57(13), pp. 5858–5878. https://doi.org/10.1080/19443994.2015.1004115.

Afshar Moghaddam, M. and Seyyedi, K., 2022. Optimization of the Sunset Yellow dye removal by electrocoagulation using a response surface method. *Water Science and Technology*, 85(1), pp. 206–219. https://doi.org/10.2166/wst.2021.500.

Al-Bayati, I.S., Waisi, B.I., Mohammed, M.A., Alobaidy, A.A. and Kadhom, M.A., 2025. Crystal violet dye removal from aqueous solution using corn silks as an environmentally friendly adsorbent. *Tikrit Journal of Engineering Sciences*, 32(2). https://doi.org/10.25130/tjes.32.2.16.

Alinejad-Mir, A., Amooey, A.A. and Ghasemi, S., 2018. Adsorption of direct yellow 12 from aqueous solutions by an iron oxide-gelatin nanoadsorbent; kinetic, isotherm and mechanism analysis. *Journal of Cleaner Production*, 170, pp. 570–580. https://doi.org/10.1016/j.jclepro.2017.09.101.

Aoyama, Y., Sato, N., Toyotama, A., Okuzono, T. and Yamanaka, J., 2022. Particle adsorption on polymer gel surface driven by van der Waals attraction. *Bulletin of the Chemical Society of Japan*, 95(2), pp. 314–324. https://doi.org/10.1246/bcsj.20210356.

Aragaw, T.A. and Alene, A.N., 2022. A comparative study of acidic, basic, and reactive dyes adsorption from aqueous solution onto kaolin adsorbent: Effect of operating parameters, isotherms, kinetics, and thermodynamics. *Emerging Contaminants*, 8, pp. 59–74. https://doi.org/10.1016/j.emcon.2022.01.002.

Aragaw, T.A., 2020. Recovery of iron hydroxides from electro-coagulated sludge for adsorption removals of dye wastewater: Adsorption capacity and adsorbent characteristics. *Surfaces and Interfaces*, 18. https://doi.org/10.1016/j.surfin.2020.100439.

Balakrishnan, B., Joshi, N. and Banerjee, R., 2013. Borate aided Schiff's base formation yields in situ gelling hydrogels for cartilage regeneration. *Journal of Materials Chemistry B*, 1(41), pp. 5564–5577. https://doi.org/10.1039/c3tb21056a.

Benjakul, S., Oungbho, K., Visessanguan, W., Thiansilakul, Y. and Roytrakul, S., 2009. Characteristics of gelatin from the skins of bigeye snapper, Priacanthus tayenus and Priacanthus macracanthus. *Food Chemistry*, 116(2), pp. 445–451. https://doi.org/10.1016/j.foodchem.2009.02.063.

Chen, Y., Feng, X. and Fu, B., 2021. An improved global remote-sensing-based surface soil moisture (RSSSM) dataset covering 2003-2018. *Earth System Science Data*, https://doi.org/10.5194/essd-13-1-2021.

Chen, Y., Ma, Y., Lu, W., Guo, Y., Zhu, Y., Lu, H. and Song, Y., 2018. Environmentally friendly gelatin/β-cyclodextrin composite fiber adsorbents for the efficient removal of dyes from wastewater. *Molecules*, 23(10). https://doi.org/10.3390/molecules23102473.

Chittur, K.K., 1998. FTIR/ATR for protein adsorption to biomaterial surfaces. *Biomaterials*, .

Chung, H.K., Kim, W.H., Park, J., Cho, J., Jeong, T.Y. and Park, P.K., 2015. Application of Langmuir and Freundlich isotherms to predict adsorbate removal efficiency or required amount of adsorbent. *Journal of Industrial and Engineering Chemistry*, 28, pp. 241–246. https://doi.org/10.1016/j.jiec.2015.02.021.

Cui, T., Sun, Y., Wu, Y., Wang, J., Ding, Y., Cheng, J. and Guo, M., 2022. Mechanical, microstructural, and rheological characterization of gelatin-dialdehyde starch hydrogels constructed by dual dynamic crosslinking. *LWT*, 161. https://doi.org/10.1016/j.lwt.2022.113374.

Dassanayake, R.S., Acharya, S. and Abidi, N., 2021. Recent advances in biopolymer-based dye removal technologies. *Molecules*, 26(15). https://doi.org/10.3390/molecules26154697.

Dawood, S., Sen, T.K. and Phan, C., 2016. Adsorption removal of Methylene Blue (MB) dye from aqueous solution by bio-char prepared from Eucalyptus sheathiana bark: Kinetic, equilibrium, mechanism, thermodynamic and process design. *Desalination and Water Treatment*, 57(59), pp. 28964–28980. https://doi.org/10.1080/19443994.2016.1188732.

De Carvalho, R.A. and Grosso, C.R.F., 2004. Characterization of gelatin based films modified with transglutaminase, glyoxal and formaldehyde. *Food Hydrocolloids*, 18(5), pp. 717–726. https://doi.org/10.1016/j.foodhyd.2003.10.005.

de Sá, F.P., Cunha, B.N. and Nunes, L.M., 2013. Effect of pH on the adsorption of Sunset Yellow FCF food dye into a layered double hydroxide (CaAl-LDH-NO3). *Chemical Engineering Journal*, 215–216, pp. 122–127. https://doi.org/10.1016/j.cej.2012.11.024.

Dey, S. and Nagababu, B.H., 2022. Applications of food color and bio-preservatives in the food and its effect on the human health. *Food Chemistry Advances*, https://doi.org/10.1016/j.focha.2022.100019.

El-Azazy, M., Dimassi, S.N., El-Shafie, A.S. and Issa, A.A., 2019. Bio-Waste Aloe vera Leaves as an efficient adsorbent for Titan Yellow from Wastewater: Structuring of a novel adsorbent using Plackett-Burman factorial design. *Applied Sciences (Switzerland)*, 9(22). https://doi.org/10.3390/app9224856.

EL-Sayed, N.S., El-Ziaty, A.K., El-Meligy, M.G. and Nagieb, Z.A., 2017. Syntheses of new antimicrobial cellulose materials based 2-((2-aminoethyl)amino)-4-aryl-6-indolylnicotinonitriles. *Egyptian Journal of Chemistry*, 60(3), pp. 465–477. https://doi.org/10.21608/ejchem.2017.3375.

Esvandi, Z., Foroutan, R., Peighambardoust, S.J., Akbari, A. and Ramavandi, B., 2020. Uptake of anionic and cationic dyes from water using natural clay and clay/starch/MnFe2O4 magnetic nanocomposite. *Surfaces and Interfaces*, 21. https://doi.org/10.1016/j.surfin.2020.100754.

Farris, S., Song, J. and Huang, Q., 2010. Alternative reaction mechanism for the cross-linking of gelatin with glutaraldehyde. *Journal of Agricultural and Food Chemistry*, 58(2), pp. 998–1003. https://doi.org/10.1021/jf9031603.

Fatombi, J.K., Idohou, E.A., Osseni, S.A., Agani, I., Neumeyer, D., Verelst, M., Mauricot, R. and Aminou, T., 2019. Adsorption of Indigo Carmine from Aqueous Solution by Chitosan and Chitosan/Activated Carbon Composite: Kinetics, Isotherms and Thermodynamics Studies. *Fibers and Polymers*, 20(9), pp. 1820–1832. https://doi.org/10.1007/s12221-019-1107-y.

Filice, S., Bongiorno, C., Libertino, S., Compagnini, G., Gradon, L., Iannazzo, D., La Magna, A. and Scalese, S., 2021. Structural characterization and adsorption properties of dunino raw halloysite mineral for dye removal from water. *Materials*, 14(13). https://doi.org/10.3390/ma14133676.

Garg, V.K., Amita, M., Kumar, R. and Gupta, R., 2004. Basic dye (methylene blue) removal from simulated wastewater by adsorption using Indian Rosewood sawdust: A timber industry waste. *Dyes and Pigments*, 63(3), pp. 243–250. https://doi.org/10.1016/j.dyepig.2004.03.005.

Hadi, S.M., Al-Mashhadani, M.K. and Eisa, M.Y., 2019. Optimization of dye adsorption process for Albizia lebbeck pods as a biomass using central composite rotatable design model. *Chemical Industry and Chemical Engineering Quarterly*, 25(1), pp. 39–46. https://doi.org/10.2298/CICEQ180210021H.

Hashemian, S., Salari, K., Salehifar, H. and Atashi Yazdi, Z., 2013. Removal of azo dyes (violet b and violet 5r) from aqueous solution using new activated carbon developed from orange peel. *Journal of Chemistry*, 2013. https://doi.org/10.1155/2013/283274.

Hiawi, F.A. and Ali, I.H., 2023. Study the interaction adsorptive behavior of sunset Yellow Dye and Loratadine Drug: Kinetics and thermodynamics study. *Ibn AL-Haitham Journal For Pure and Applied Sciences*, 36(1), pp. 186–196. https://doi.org/10.30526/36.1.2974.

Hu, Q.H., Qiao, S.Z., Haghseresht, F., Wilson, M.A. and Lu, G.Q., 2006. Adsorption study for removal of basic red dye using bentonite. *Industrial and Engineering Chemistry Research*, 45(2), pp. 733–738. https://doi.org/10.1021/ie050889y.

Imani, R., Rafienia, M. and Emami, S.H., 2013. Synthesis and characterization of glutaraldehyde-based crosslinked gelatin as a local hemostat sponge in surgery: an in vitro study. *Bio-medical materials and engineering*, 23(3), pp. 211–224. https://doi.org/10.3233/bme-130745.

Kakavandi, B., Takdastan, A., Pourfadakari, S., Ahmadmoazzam, M. and Jorfi, S., 2019. Heterogeneous catalytic degradation of organic compounds using nanoscale zero-valent iron supported on kaolinite: Mechanism, kinetic and feasibility studies. *Journal of the Taiwan Institute of Chemical Engineers*, 96, pp. 329–340. https://doi.org/10.1016/j.jtice.2018.11.027.

Kalash, K.R., Alalwan, H.A., Al-Furaiji, M.H., Alminshid, A.H. and Waisi, B.I., 2020. Isothermal and kinetic studies of the adsorption removal of Pb(II), Cu(II), and Ni(II) Ions from Aqueous Solutions using Modified Chara Sp. Algae. *Korean Chemical Engineering Research*, 58(2), pp. 301–306. https://doi.org/10.9713/kcer.2020.58.2.301.

Kong, Q., Liu, Q., Miao, M.S., Liu, Y.Z., Chen, Q.F. and Zhao, C.S., 2017. Kinetic and equilibrium studies of the biosorption of sunset yellow dye by alligator weed activated carbon. *Desalination and Water Treatment*, 66, pp. 281–290. https://doi.org/10.5004/dwt.2017.20223.

Lata, H., Garg, V.K. and Gupta, R.K., 2007. Removal of a basic dye from aqueous solution by adsorption using Parthenium hysterophorus: An agricultural waste. *Dyes and Pigments*, 74(3), pp. 653–658. https://doi.org/10.1016/j.dyepig.2006.04.007.

Li, D., Ye, Y., Li, D., Li, X. and Mu, C., 2016. Biological properties of dialdehyde carboxymethyl cellulose crosslinked gelatin-PEG composite hydrogel fibers for wound dressings. *Carbohydrate Polymers*, 137, pp. 508–514. https://doi.org/10.1016/j.carbpol.2015.11.024.

Li, G., Jiang, Y., Li, M., Zhang, W., Li, Q. and Tang, K., 2021. Investigation on the tunable effect of oxidized konjac glucomannan with different molecular weight on gelatin-based composite hydrogels. *International Journal of Biological Macromolecules*, 168, pp. 233–241. https://doi.org/10.1016/j.ijbiomac.2020.12.056.

Li, W., Ma, Q., Bai, Y., Xu, D., Wu, M. and Ma, H., 2018. Facile fabrication of gelatin/bentonite composite beads for tunable removal of anionic and cationic dyes. *Chemical Engineering Research and Design*, 134, pp. 336–346. https://doi.org/10.1016/j.cherd.2018.04.016.

Maroufi, L.Y., Shahabi, N., Ghanbarzadeh, M. dokht and Ghorbani, M., 2022. Development of antimicrobial active food packaging film based on Gelatin/Dialdehyde quince seed gum incorporated with Apple Peel Polyphenols. *Food and Bioprocess Technology*, 15(3), pp. 693–705. https://doi.org/10.1007/s11947-022-02774-8.

Masri, S., Maarof, M., Mohd, N.F., Hiraoka, Y., Tabata, Y. and Fauzi, M.B., 2022. Injectable Crosslinked Genipin Hybrid Gelatin–PVA Hydrogels for future use as Bioinks in Expediting Cutaneous Healing Capacity: Physicochemical Characterisation and Cytotoxicity Evaluation. *Biomedicines*, 10(10). https://doi.org/10.3390/biomedicines10102651.

Michelini, L., Probo, L., Farè, S. and Negrini, N.C., 2020. Characterization of gelatin hydrogels derived from different animal sources. *National Interuniversity Consortium of Materials Science and Technology*, 272. https://doi.org/10.1016/j.matlet.2020.127865.

Mohammed, M.A., Al-Bayati, I.S., Alobaidy, A.A., Waisi, B.I. and Majeed, N., 2023. Investigation the efficiency of emulsion liquid membrane process for malachite green dye separation from water. *Desalination and Water Treatment*, 307, pp. 190–195. https://doi.org/10.5004/dwt.2023.29903.

Mokrejš, P., Mrázek, P., Gál, R. and Pavlačková, J., 2019. Biotechnological preparation of gelatines from chicken feet. *Polymers*, 11(6). https://doi.org/10.3390/POLYM11061060.

Mugnaini, G., Gelli, R., Mori, L. and Bonini, M., 2023. How to cross-link Gelatin: The effect of Glutaraldehyde and Glyceraldehyde on the Hydrogel properties. *ACS Applied Polymer Materials*, 5(11), pp. 9192–9202. https://doi.org/10.1021/acsapm.3c01676.

Pal, K., Paulson, A.T. and Rousseau, D., 2009. Biopolymers in controlled-release delivery systems. In: *Modern Biopolymer Science*. Academic Press. pp. 519–557. https://doi.org/10.1016/B978-1-4557-2834-3.00014-8.

Panić, V. V., Šešlija, S.I., Nešić, A.R. and Veličković, S.J., 2013. Adsorption of azo dyes on polymer materials. *Hemijska Industrija*, 67(6), pp. 881–900. https://doi.org/10.2298/HEMIND121203020P.

Piccin, J.S., Gomes, C.S., Feris, L.A. and Gutterres, M., 2012. Kinetics and isotherms of leather dye adsorption by tannery solid waste. *Chemical Engineering Journal*, 183, pp. 30–38. https://doi.org/10.1016/j.cej.2011.12.013.

Prashanna Suvaitha, S. and Venkatachalam, K., 2023. Isotherms, kinetics, and thermodynamics adsorption of sunset yellow, indigo carmine, titan yellow, and orange G with Polyvinylpyrrolidone-Aminopropyl-SBA-15 schiff base. *Water, Air, and Soil Pollution*, 234(8). https://doi.org/10.1007/s11270-023-06510-6.

Ramalakshmi, S., Muthuchelian, K. and Swaminathan, K., 2011. Kinetic and equilibrium studies on biosorption of reactive orange 107 dye from aqueous solution by native and treated fungus Alternaria Raphani. *J. Chem. Pharm. Res*, 3(6), pp. 337–347.

Ren, J., Wang, X., Zhao, L., Li, M. and Yang, W., 2021. Effective removal of dyes from aqueous solutions by a Gelatin Hydrogel. *Journal of Polymers and the Environment*, 29(11), pp. 3497–3508. https://doi.org/10.1007/s10924-021-02136-z.

Sacks, M.S., Gorman, R.C., Hamamoto, H., Connolly, J.M., Gorman Iii, J.H. and Levy, R., 2007. In vivo biomechanical assessment of trigycidylamine crosslinked pericardium. *Biomaterials*, 28(35), pp. 5390–5398. https://doi.org/10.1016/j.biomaterials.2007.08.021.

Salvi, N.A. and Chattopadhyay, S., 2017. Biosorption of Azo dyes by spent Rhizopus arrhizus biomass. *Applied Water Science*, 7(6), pp. 3041–3054. https://doi.org/10.1007/s13201-016-0417-0.

Sen, T.K., Thi, M.T., Afroze, S., Phan, C. and Ang, M., 2012. Removal of anionic surfactant sodium dodecyl sulphate from aqueous solution by adsorption onto pine cone biomass of Pinus Radiate: equilibrium, thermodynamic, kinetics, mechanism and process design. *Desalination and Water Treatment*, 45. https://doi.org/10.1080/19443994.2012.692036.

Sethi, S., Kaith, B.S., Kaur, M., Sharma, N. and Khullar, S., 2020. A hydrogel based on dialdehyde carboxymethyl cellulose–gelatin and its utilization as a bio adsorbent. *Journal of Chemical Sciences*, 132(1). https://doi.org/10.1007/s12039-019-1700-z.

Shahryari, Z., Goharrizi, A.S. and Azadi, M., 2010. Experimental study of methylene blue adsorption from aqueous solutions onto carbon nano tubes. *International Journal of Water Resources and Environmental Engineering*, 2(2), pp. 16–28. https://doi.org/10.5897/IJWREE.9000021.

Shakoor, S. and Nasar, A., 2016. Removal of methylene blue dye from artificially contaminated water using citrus limetta peel waste as a very low cost adsorbent. *Journal of the Taiwan Institute of Chemical Engineers*, 66, pp. 154–163. https://doi.org/10.1016/j.jtice.2016.06.009.

Sun, D., Zhang, X., Wu, Y. and Liu, X., 2010. Adsorption of anionic dyes from aqueous solution on fly ash. *Journal of Hazardous Materials*, 181(1–3), pp. 335–342. https://doi.org/10.1016/j.jhazmat.2010.05.015.

Takdastan, A., Pourfadakari, S., Yousefi, N. and Orooji, N., 2020. Removal of sunset yellow dye using heterogeneous catalytic degradation with magnetic Fe3O4 /persulfate/ultrasound system. *Desalination and Water Treatment*, 197, pp. 402–412. https://doi.org/10.5004/dwt.2020.25956.

Tkaczyk, A., Mitrowska, K. and Posyniak, A., 2020. Synthetic organic dyes as contaminants of the aquatic environment and their implications for ecosystems: A review. *Science of the Total Environment*, 717. https://doi.org/10.1016/j.scitotenv.2020.137222.

Ulfa, M., Prasetyoko, D., Trisunaryanti, W., Bahruji, H., Fadila, Z.A. and Sholeha, N.A., 2022. The effect of gelatin as pore expander in green synthesis mesoporous silica for methylene blue adsorption. *Scientific Reports*, 12(1). https://doi.org/10.1038/s41598-022-19615-5.

Vadivelan, V. and Vasanth Kumar, K., 2005. Equilibrium, kinetics, mechanism, and process design for the sorption of methylene blue onto rice husk. *Journal of Colloid and Interface Science*, 286(1), pp. 90–100. https://doi.org/10.1016/j.jcis.2005.01.007.

Wang, Q., Yan, S., Zhu, Y., Ning, Y., Chen, T., Yang, Y., Qi, B., Huang, Y. and Li, Y., 2024. Crosslinking of gelatin Schiff base hydrogels with different structural dialdehyde polysaccharides as novel crosslinkers: Characterization and performance comparison. *Food Chemistry*, 456. https://doi.org/10.1016/j.foodchem.2024.140090.

Yinghua, S., Rong, P., Lili, G. and Mei, Y., 2021. Removal of Sunset Yellow by Methanol modified walnut shell. *J. Chem. Chem. Eng. Research Article*, 40(4). https://doi.org/10.30492/ijcce.2020.101424.3429.

Zhang, L., Liu, J., Zheng, X., Zhang, A., Zhang, X. and Tang, K., 2019. Pullulan dialdehyde crosslinked gelatin hydrogels with high strength for biomedical applications. *Carbohydrate Polymers*, 216, pp. 45–53. https://doi.org/10.1016/j.carbpol.2019.04.004.

Zhu, Y., Zhang, D., He, S., Huang, Z., Zhang, Z., Zhu, J. and Cao, Y., 2019. Controlled release of methylene blue from glutaraldehyde-modified gelatin. *Journal of Food Biochemistry*, 43(9). https://doi.org/10.1111/jfbc.12977.

جيلاتين مُعدَّل بالتشابك لإزالة الصبغة الصفراء: التحضير، التوصيف، وتقييم الأداء

هيا مصعب[1]،*، محمود المشهداني[1]، سناء الصاحب[2]

[1]قسم الهندسة الكيمياوية، كلية الهندسة، جامعة بغداد، بغداد، العراق
[2]قسم الكيمياء، كلية العلوم للبنات، جامعة بغداد، بغداد، العراق

الخلاصة

يُعدّ الجيلاتين مادة قيّمة تتميز ببنية ثلاثية الأبعاد معقدة ,غير أنها تعاني من محدودية كفاءة الامتزاز ، مما يحدّ من تطبيقاتها عند درجة الحرارة الفسيولوجية. في هذه الدراسة، تم تحسين الجيلاتين بإضافة الجلوتارالدهيد (GTA) لتعزيز قدرته على امتزاز الأصباغ من المياه الملوثة. أُجريت تجارب الامتزاز تحت ظروف مختلفة شملت كمية المادة المازّة المضافة، وتركيز الصبغة الابتدائي، ودرجة الحرارة. وأظهرت النتائج أن (qe) ازدادت مع ارتفاع التراكيز الابتدائية للصبغة، إذ تراوحت بين 4.978-23.056mg/g لـ GTA-GE، وبين 4.8-21.333 mg/g لـ GE، في حين تنخفض بزيادة كمية المادة المازّة المستخدمة. تم تحقيق حالة الاتزان عند قيمة pH مقدارها 4، وكمية مادة مازّة مقدارها 100 ملغم، خلال زمن تماس بلغ 80 دقيقة. وتراوحت كفاءة إزالة الصبغة بين 88.4–99.8% للجيلاتين المتشابك بالجلوتارالدهيد، وبين 83–96% للجيلاتين غير المعدّل. تم تحليل بيانات الاتزان باستخدام نموذجي Freundlich وLangmuir للامتزاز، وأظهر نموذج Freundlich أفضل مطابقة للبيانات(R^2= 0.995)، مما يدل على امتزاز غير متجانس متعدد الطبقات. كما أظهرت دراسة الحركية أن امتزاز صبغة الصفراء على الجيلاتين يتبع نموذج pseudo-second order (R^2= 0.981)، مما يعكس عملية امتزاز ذات كفاءة عالية. وأوضحت الديناميكية الحرارية أن أن القيمة السالبة لـ ΔG تؤكد أن العملية تلقائية وممكنة الحدوث، فيما تدل القيمة السالبة لـ ΔH (12.693kJ/mol) على أن عملية الامتزاز طاردة للحرارة. وتشير القيمة السالبة لـ ΔS (0.021kJ/k. mol) إلى انخفاض العشوائية عند السطح البيني الصلب–السائل أثناء عملية الامتزاز.كما بيّنت النتائج إمكانية إعادة استخدام المادة المازّة لأربع دورات متتالية مع انخفاض ملحوظ في كفاءة الإزالة.

الكلمات المفتاحية: جيلاتين، امتزاز، الصبغة الصفراء، الحركية، جلوتارالدهيد.